Label-free detection of cytokines using optical microcavities

Andrea M. Armani, Scott E. Fraser

Andrea M. Armani, Scott E. Fraser, "Label-free detection of cytokines using optical microcavities," Proc. SPIE 6862, Single Molecule Spectroscopy and Imaging, 68620C (21 February 2008); doi: 10.1117/12.761002

SPIE.

Event: SPIE BiOS, 2008, San Jose, California, United States

Label-free detection of cytokines using optical microcavities

Andrea M. Armani[1], Scott E. Fraser[1,2]
[1]*Department of Applied Physics, California Institute of Technology*
[2]*Division of Biology, California Institute of Technology*
1200 E California Blvd, Pasadena, CA 91125
armani@caltech.edu, sefraser@caltech.edu

ABSTRACT

Ultra-high-Q microresonators have demonstrated sensitive and specific chemical and biological detection. The sensitivity is derived from the long photon lifetime inside the cavity and specificity is achieved through surface functionalization. Here, ultra-high-Q microcavities demonstrate label-free, single molecule detection of Interleukin-2 (IL-2) in fetal bovine serum (FBS). IL-2 is a cytokine released in response to immune system activation. The surface of the microtoroids was sensitized using anti-IL-2. The detection mechanism relies upon a thermo-optic mechanism to enhance resonant wavelength shifts induced through binding of a molecule.

1. INTRODUCTION

Currently, cell biologists use several different in vitro and in vivo techniques to extract information about a cell's behavior: labeling several independent proteins and monitoring their behavior using microscopy[1, 2], lysing cells and using complimentary techniques like polymerase chain reaction (PCR) and enzyme linked immunoassays (ELISA) to determine the cells' components[3], and knocking out genes and watching for a loss of function or life (in some instances).[4] While all of these techniques have been very successful, they give indirect evidence of the information that the biologists are looking for, in the previous examples, cell signaling pathways. To solve this problem, it is necessary to develop improved sensing technologies which can provide the direct evidence needed. The new technologies need to incorporate several features: bio-compatibility, sensitivity, and specificity.

Optical microcavities have successfully demonstrated all three requirements.[5] Biocompatibility is achieved through the choice of fabrication materials. Typically, ultra-high-Q microresonators are fabrication from silica and/or silicon which are both stable in a wide range of environments. Sensitivity is inherent to ultra-high-Q microcavities because of the long photon lifetime within the microcavity which results in an increase in sampling.[6] This ability allows microcavities to perform detection experiments without labeling the target molecules. All other sensors which are capable of performing single molecule detection experiments require that the target is labeled with a fluorescent probe.[7] Additionally, microcavity-based detection can be performed in real-time, which allows for data to be taken continuously while other biologically relevant parameters (such as temperature, pH, salt) are changed. Specificity is endowed to the microcavity through surface functionalization.[8]

Previous microcavity detection experiments have been performed using a range of geometries and materials.[9] Silica resonant sensors fabricated from high-Q microspheres (Q~2 million) have demonstrated the ability to distinguish between two strands of DNA and between cis/trans isomers based on a resonant wavelength shift in real time. [10, 11] The Q in these experiments was limited by the testing wavelength and was not a fundamental limit of the cavity. Polymer devices have also performed similar biological detection experiments. Polymer microring resonators have demonstrated detection of glucose.[12, 13] The techniques used to fabricate these devices enable integration and multiplexing.[14] Integrated polymer resonator sensors

Single Molecule Spectroscopy and Imaging
edited by Jörg Enderlein, Zygmunt K. Gryczynski, Rainer Erdmann
Proc. of SPIE Vol. 6862, 68620C, (2008) · 1605-7422/08/$18 · doi: 10.1117/12.761002

have also demonstrated detection of avidin[15] The quality factors of the polymer devices were limited by the fabrication methods used.[16]

An alternative technique is to fabricate a resonant cavity laser and monitor the lasing wavelength.[17] This method allows a lower Q cavity to perform with similar sensitivity to a higher Q cavity, based upon the lasing linewidth. Resonant laser sensors have been successfully demonstrated using photonic crystals and microdisk lasers. While the strength of the microcavity is its ability to perform label-free detection experiments, labeled experiments can also be performed.[18] In these experiments, the resonant wavelength of the cavity is used as the excitation source, and only molecules sufficiently close to the cavity are excited. These types of experiments are especially suited for Fabry-Perot resonators which typically have lower quality factors and would otherwise have difficulty performing single molecule experiments[19].

Single molecule experiments using ultra-high-Q resonators have been previously proposed using a variety of detection techniques such as fluorescence [18], transmission variations [6] and polarizability changes[20]. However, these mechanisms incorrectly assumed that the molecule was non-absorbing. As has been shown in previous theoretical and experimental studies, an absorbing monolayer will have significant effects on a microcavity's behavior [21-23].

Spectrophotometer measurements across the visible spectrum are regularly performed in biology laboratories to measure the concentration (M) of a solution of biological molecules.[24] This type of measurement would not be accurate if the molecules did not absorb at these wavelengths. These losses interact with the whispering gallery mode of the microcavity and, due to the high circulating intensities present in the microcavity, are amplified. The subsequent heating of the microcavity induces a resonant wavelength red-shift which can be described by the thermo-optic effect. This effect has not been previously proposed as a detection mechanism because of the incorrect assumption that biological molecules were non-absorbing.

The thermo-optic effect has been used previously in designing tunable microresonator devices [25, 26]. In these previous devices, the heat source was typically a metallic contact near the resonant cavity or an electrically conducting polymer. In a biological sensor, the heat source is the molecule being detected. Because the molecule has a higher material absorption than either the water or the silica, as it interacts with the whispering gallery mode, the molecule absorbs light and increases in temperature. This heat is then conducted to the resonant cavity. The amount of heat that the molecule generates is dependent on the material absorption of the molecule, which is easily determined using a commercially available spectrophotometer, and on several other parameters, such as input power, Q and mode volume. In microcavity-based detection, the microcavity directly detects the molecule. This direct detection is in contrast to the previous single molecule experiments based on fluorescent labels, where the emission of light from the label is detected, not the molecule. As will be shown, while both the silica microsphere[21] and microtoroid[27] resonators have achieved quality factors great than 100 million in air, the microtoroid is better suited for biological sensing because of the reduced mode volume.

From finite element modeling (FEM) of microtoroid resonators, it has been shown that the majority of the optical field intensity (over 90%) resides within the silica. Additionally, the conductivity of water and silica are similar (0.6 and 1.38 W/m °K). Taking both of these into account and beginning with the wave equation and adding a perturbing thermal contribution to the susceptibility, the theoretical wavelength shift produced by a single bound molecule via the thermo-optic mechanism can be shown to be given by the expression below:

$$\left[\frac{\delta\lambda}{\lambda}\right]_{SM} = \frac{\sigma\,\lambda\,{}^{dn}\!/_{dT}}{8\pi^2 n^2 \kappa V} QP \int \frac{|u(\vec{r})|^2}{|\vec{r}|+\varepsilon} d\vec{r} \qquad (1)$$

where λ is the wavelength, σ is the absorption cross section of a single molecule, *dn/dT* is the opto-thermal constant of silica ($1.3\text{x}10^{-5}$ K^{-1}), κ is thermal conductivity, *n* is the effective refractive index of the silica toroid, *V* is the optical mode volume, *Q* is cavity Q-factor, and *P* is the coupled optical power. The integral in this expression accounts for the spatial overlap of the whispering gallery mode field ($u(\vec{r})$) with the temperature profile created by the nearly point-like molecular heat source.

The actual form of the temperature plume in the vicinity of the molecule is likely complex and has been combined into a single empirical parameter, ε. In contrasting a perfect point source of heat with a molecule, this parameter captures the essential fact that the temperature profile is not singular at the source and instead rises steadily until reaching some radius of order the molecular size. This approximation is justified first because the thermal transport process itself rapidly smoothes nano-scale spatial variations created by molecular shape, and second because the ensuing temperature field created by the molecular hot spot is long-range (i.e., 1/r dependence). For this reason, the tuning shift is only a weak function of the parameter "ε". In fact, a variation in "ε" of 1 nm to 100 nm induces only a 16% change in resonant wavelength shift. Therefore, the optical cross section σ is more significant to the thermo-optic induced heating that the physical radius, ε. On the other hand, the size of "ε" strongly suggests a maximum temperature in the vicinity of the molecule. Additionally, we expect "ε" to be many times the actual physical size of the molecule. Since "ε" is an empirical parameter of which relatively little is known, we will provide all calculations over a range of "ε" encompassing the molecular width to a size that is 100 times as large as this width.

Using this expression, it is also possible to establish a minimum absorption-cross-section sensitivity by setting the observed shift equal to the cavity linewidth:

$$\sigma_{\min} = \frac{V}{Q^2}\frac{1}{P}\frac{8\pi^2 n^2 \kappa}{\lambda\,{}^{dn}\!/_{dT}}\left[\int \frac{|u(\vec{r})|^2}{|\vec{r}|+\varepsilon} d\vec{r}\right]^{-1} \qquad (2)$$

This expression also illustrates a key point made earlier that the sensitivity benefits quadratically from the cavity Q factor. As an example, for a cavity Q factor of 250 million, a coupled power of 1 mW, a molecular radius in the range of 3-50 nm, a wavelength of 670 nm, a toroid of diameter 80 microns, and using optical and thermal constants of silica, we would predict a absorption-cross-section limit between $1.1\text{x}10^{-17}$ cm^2 and $1.5\text{x}10^{-17}$ cm^2. Typical absorption cross section values for antigens, which are some of the smallest molecules of interest to biologists, are $\sim 10^{-16}$ cm^2. Therefore, the absorption cross section limit using the microtoroid resonator is well below these values, and furthermore, represents only the limit one would encounter using resonance-shift detection methods sensitive only to shifts of order the resonator linewidth. If a cross section of $2\text{x}10^{-16}$ cm^2 is assumed, then a single molecule wavelength shift of between 50 fm and 33 fm is predicted, which is easily detected using an ultra-high Q toroidal microcavity[27, 28]. The small range of variation here (in predicted wavelength shift) illustrate the relative insensitivity of each of these quantities to the parameter, ε.

However, often reverse detection, or detection of the antibody, can be useful in revealing information about a biological system. These molecules are over an order of magnitude larger, typically $\sim 10^{-15}$ cm^2. Therefore, in generalizing this detection mechanism to other resonant cavities, it is important to determine the minimum requirements for detection of both antigens and antibodies. Additionally, the dependence on mode volume, thermal conductivity, refractive index, opto-thermal constant, and power in (2) can often compensate for a

lower Q factor. In a sense, a resonator's design can be optimized for detection, just as it would be for other applications.

Two interesting examples are the ultra-high-Q microsphere and the high-Q polymer microring resonator. It might be assumed that the ultra-high-Q microsphere should also be able to achieve the same sensitivity levels as the microtoroid, because they have similar Q factors. Additionally, since they are both fabricated from silica, they have identical thermo-optic coefficients, refractive indices, and thermal conductivities. However, as alluded to previously, because of the increase in the mode volume ($2000\mu m^3$) due to the significant increase in diameter over the microtoroid, the sensitivity decreases by over an order of magnitude. Therefore, while the microsphere is still able to detect antibodies at the single molecule level using 1mW input power, it requires 10mW input power to detect antigens at the single molecule level, despite having Q>100 million. Conversely, because the cavity Q decreases to 10^5 when resonators are fabricated out of polymeric materials [12, 29] (such as PMMA), single molecule sensitivity has never been proposed with these devices. However, it is possible to achieve single molecule antigen detection with 10mW of input power, the same as the silica microspheres. This sensitivity is directly related to the low thermal conductivity (0.2 W/m K), high refractive index (1.45) and high thermo-optic co-efficient ($1.0x10^{-4}$ K^{-1}) of PMMA and the small mode volume ($0.21\mu m^3$) of the resonator.

2. METHODOLOGY

A single-mode, tunable external cavity laser centered at 681.5nm was coupled to a single-mode tapered optical fiber waveguide. Tapered optical fibers are very low-loss/high-efficiency waveguides used for probing ultra-high-Q modes in microcavities (Figure 1).[30] To create the testing chamber, the UHQ microtoroids were placed on a high-resolution translation stage and were monitored by two cameras (top and side view) simultaneously. With the taper waveguide in close proximity to the microtoroid, pure water was added and a cover slip was placed on top, forming a water-filled microaquarium.[28] Solutions were injected into the aquarium and removed from the aquarium using a series of syringes at one end. Both the intrinsic Q and resonant wavelength were determined by monitoring the power transmission spectra. The intrinsic Q factor was determined by scanning the wavelength of the single-mode laser and measuring both the resonant power transmission and the loaded linewidth (full-width-half-maximum) in the under-coupled regime. The intrinsic modal linewidth (and hence intrinsic Q) is then computed using a resonator-waveguide coupling model. [30, 31] The position of the resonant frequency was determined by scanning the laser over a 0.03nm range and recording the resonance position from an oscilloscope.

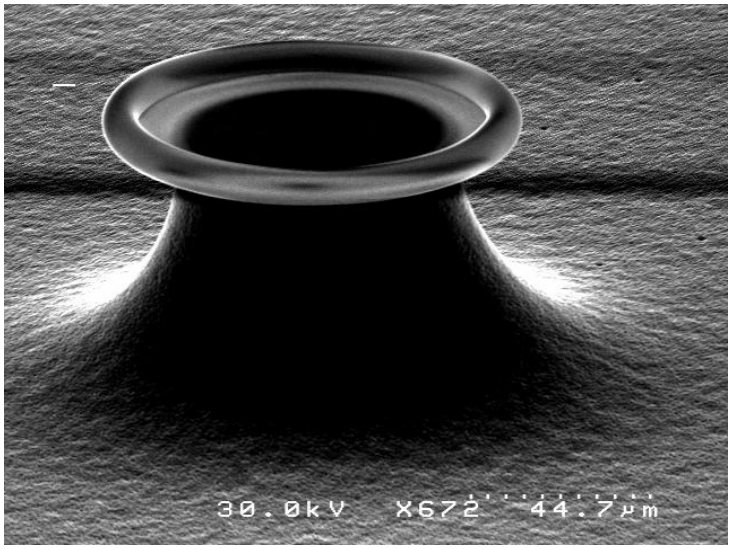

Figure 1: Scanning electron micrograph of a toroidal resonator.

A Biotin surface functionalization was used. To detect Streptavidin, the surface of the toroid was functionalized with 0.1 μM of Biotin. The large dissociation constant (K_D) of the Streptavidin-Biotin bond has increased its popularity among biologists and biochemists, and it is commonly used to functionalize sensor surfaces.[32] Additionally, because antibodies can be easily biotinylated, this technique creates a "self-passivating" surface or one where only the antibody with the Biotin-tag on it binds to the surface. Finally, studies have shown that the Biotin-Streptavidin pair correctly align and orient antibodies on a silica surface.[8] Therefore, this pair of functionalization techniques forms a foundation for a vast array of future experiments in this field.

To perform single molecule measurements, a $3x10^{-16}$ M (300aM) solutions of the target molecule (Streptavidin) were used. At this concentration level, only a few molecular binding events on the whispering gallery are expected. As this solution was added, the resonance position was recorded using an automated data acquisition system until the 1mL syringe was empty. The solution around the toroid was then cleansed by removing the ambient solution and replacing it with fresh water. At this concentration, single molecule detection experiments could be repeated numerous times on a single microtoroid.

To verify this opto-thermal theory and its dependence on the resonant cavity's quality factor, a series of single-molecule experiment were performed using the microtoroid resonant cavity sensor. The surface of the toroid was first sensitized with Protein G to perform single molecule detection of an Interleukin-2 polyclonal antibody (Invitrogen). Interleukin-2 (IL-2) is a cytokine that that is involved in regulating T-cell production.

3. RESULTS

An example of single molecule detection is shown in Figure 2a for two different cavity Q factors, $Q=1x10^8$ and $Q=2x10^8$. As molecules bind to the surface of the microtoroid, the resonant wavelength red shifts. Step-wise shifts are easily observed because the data acquisition rate, solution injection rate and the solution concentration were appropriately chosen. Using this data, a histogram of the distribution of shifts is plotted in Figure 2b (bin size is 0.01 pm). The range in shifts is a result of molecules binding throughout the whispering gallery mode and interacting with a range in optical intensities. The largest shift represents the case when the molecule binds at the highest optical field intensity. It is important to note that the largest shift which occurs

in the case when the Q~2E8 is nearly twice that in the case of Q~1E8. The thermo-optic detection mechanism predicted shift for an IL-2 antibody (cross section $\sigma=1.97\text{x}10^{-15}\text{cm}^2$) with Q values [$1\text{x}10^8$, $2\text{x}10^8$] is [0.25, 0.50] pm; the experimental shifts shown in Figure 2b are in very good agreement with this mechanism ($\Delta\lambda$=[0.23, 0.46] pm).

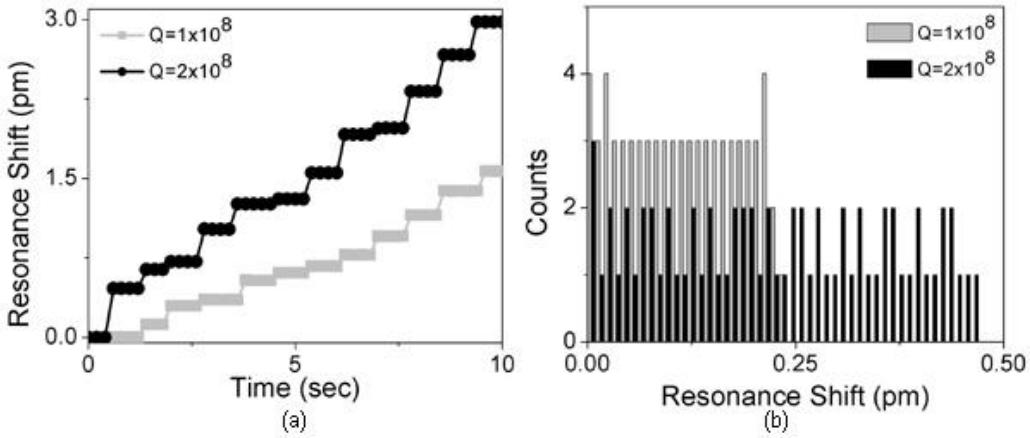

Figure 2: Single molecule detection of anti-IL-2 using the microtoroid sensor with a Q of $1\text{x}10^8$ (gray) or $2\text{x}10^8$ (black). a) As molecules bind to the surface, the resonant wavelength red-shifts, creating the steps seen. b) Two histograms created from the resonant wavelength shift data. The largest shift results from a molecule binding at the highest intensity region of the microtoroid. The maximum shift recorded using a toroid with a Q of $2\text{x}10^8$ was proportionally larger than those achieved using a toroid with a Q of $1\text{x}10^8$. The bin size of the histogram is 0.01pm.

The second experiment focused on the relationship between resonant wavelength shift and cavity Q. As the cavity Q increases from 2 million to 200 million, the resonant wavelength shift increases linearly (Figure 3). Only the largest wavelength shift for each Q factor which corresponds to when a polyclonal anti-IL2 molecule binds at the highest intensity region on the microtoroid, as determined from a histogram similar to Figure 2b, are plotted on this graph. The theoretical prediction based upon the thermo-optic detection mechanism is also included in Figure 5, and there is excellent agreement.

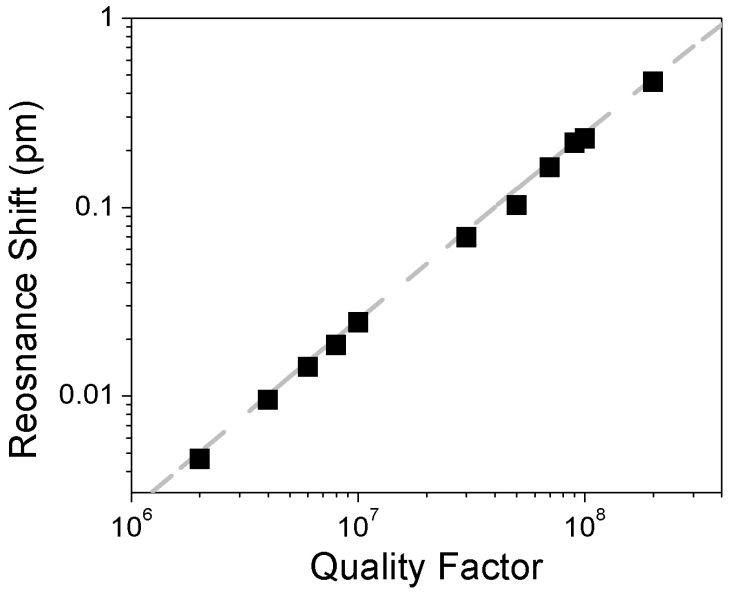

Figure 3: Resonant wavelength shift as a function of quality factor. As the quality factor of the toroidal resonator increases, the resonant wavelength shift increases. Therefore, a higher Q cavity is able to detect smaller species. The theoretical prediction based upon the thermo-optic mechanism is shown (red line). The absorption cross section of the polyclonal anti-IL-2 used in this study is $1.9 \times 10^{-15} cm^2$.

While the microtoroid resonator is able to easily perform these label-free, single molecule experiments over a range of Q factors, it is important to note that this ability is possible in other resonant cavities if they are optimized for detection.

Additional experiments were performed to investigate the suitability of the microtoroid resonator in a real-life application. IL-2 is a cytokine which is released in response to immune system activation. However, the concentration of IL-2 in serum has been shown to change in patients with childhood leukemia and to be an indicator of an impaired immune system.[33] However, IL-2 is present in serum at very low concentrations (10^{-12}-10^{-15}M) and therefore, it can be difficult to be able to monitor these changes quickly.

The surface of the resonator was functionalized with anti-IL-2 for detection of IL-2. A series of IL-2 solutions ranging from 100aM to 900aM in buffer and in serum were made. By optimizing solution concentration, solution injection rate, and data acquisition rate, shifts caused by individual molecules binding to the surface of the toroid were resolved. Step-wise shifts in buffer and in serum were observed (Figure 4), and their frequency scaled linearly with concentration.

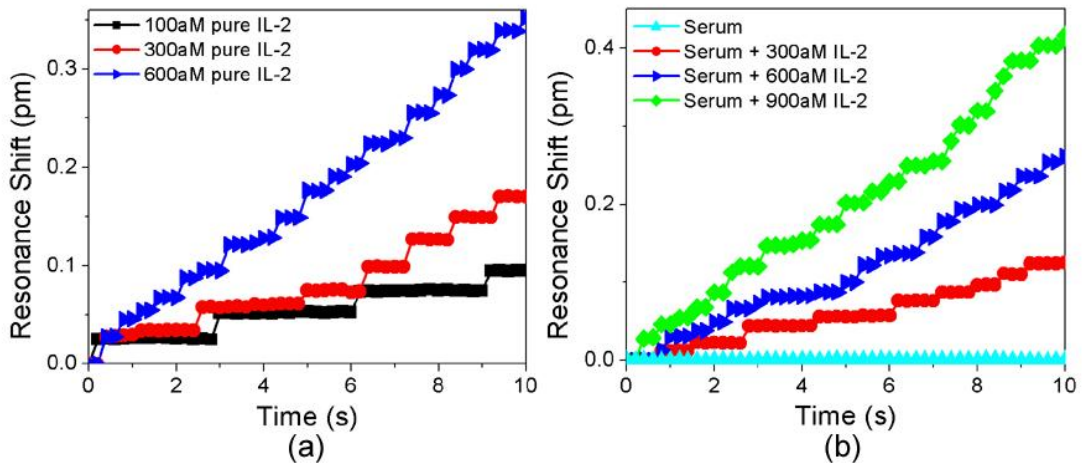

Figure 4: The position of the resonance wavelength as a function of time at three different Interleukin-2 concentrations (a) in buffer) and (b) in serum. As molecules bind to the surface, the resonant wavelength position jumps, creating the steps seen. When the concentration is increased, the general slope of the trace increased because the binding rate increased. It is important to note that discrete binding events can be resolved at this data acquisition rate. Also shown is the case of pure serum.

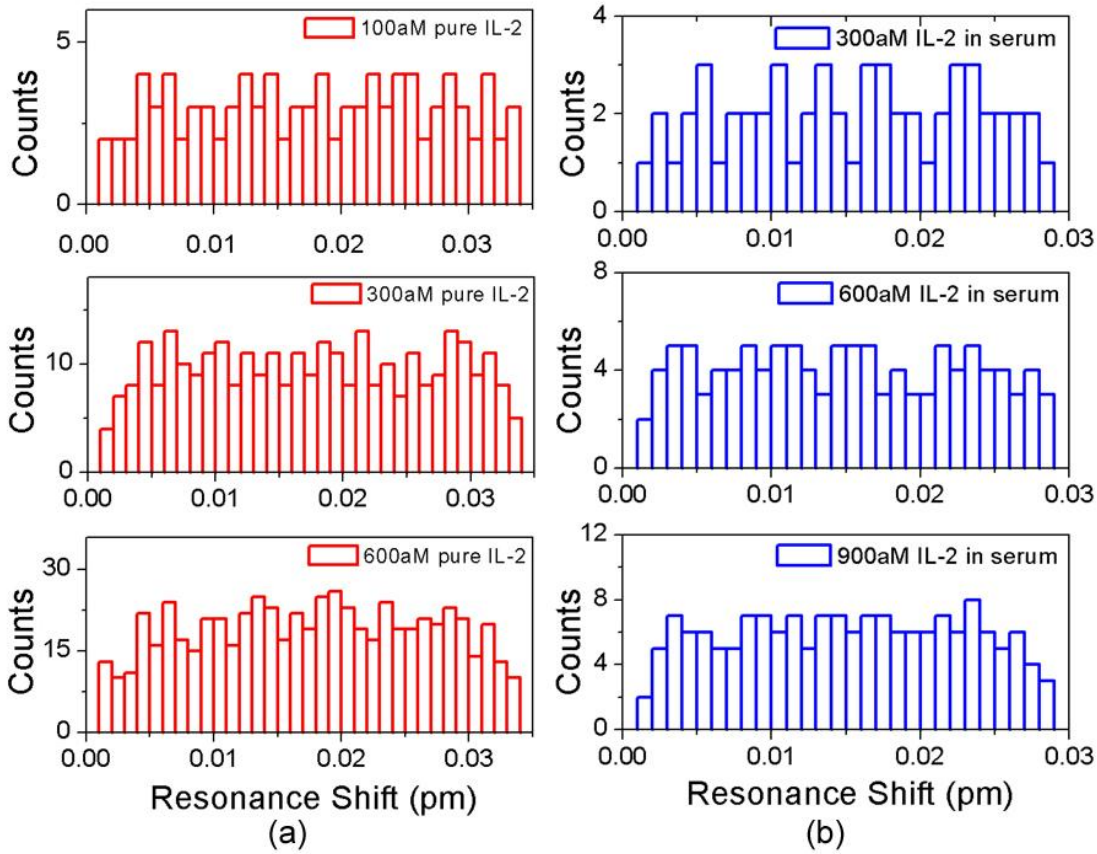

Figure 5: A series of histograms formed from steps like those in Figure 4 showing the relation between total resonant wavelength shift and number of molecules which bound to the

surface of the toroid (a) in buffer and (b) in serum. As the concentration increased, the number of binding events increased; however, the largest shift remained constant. This shift is a result of molecules binding at the highest intensity region on the surface of the toroid. The largest shift achieved agrees very well with the expected shift from the thermo-optic theory based on the quality factor of the microcavity used in this experiment (1.20×10^8 for buffer and 1.05×10^8 for serum). The bin size is 0.001pm.

The histogram of the distribution of shifts over a given period of time is plotted in Fig. 5 for several concentrations of IL-2 in buffer or in serum (bin size is 0.001 pm). In each case, the histogram has a maximum shift value that is independent of the concentration. This behavior is expected because the maximum shift is independent of concentration (as long as single molecule events are being resolved). The interaction will be strongest for binding at the equatorial plane and diminish rapidly. Hence, these histogram plots are consistent with somewhat uniform binding of molecules over the toroid surface.

There are several features of this data which are significant: the total resonant wavelength shift/number of binding events increases in proportion to the concentration, the individual binding events can be resolved and the shift from the pure serum is negligible indicating that none of the additional components in the serum interferes significantly with the detection.

4. CONCLUSION

While optical resonators offer sensitivity enhancements over alternative techniques, they also offer numerous opportunities for integration, including fluidic, optical and electrical controls.

For example, an area of future growth will be the incorporation of microfluidic controls which will allow for directed delivery of small volumes of reagents to the resonator's surface. This technique will also significantly reduce the amount of liquid necessary for detection and the time required for individual experiments.

In the present work, wavelength scanning of a high Q resonance is accomplished by using a tunable laser. However, tunable high-Q resonators have been demonstrated [26, 34, 35], and if used as biosensors, would enable a fixed wavelength optical source. This type of source could potentially be heterogeneously integrated onto the silicon chip thereby further miniaturizing the chemical and biological detector.

There is currently great interest in resonator-based detectors as they offer enhanced sensitivity in a micro-scale form factor. The work presented here has shown how silica toroidal devices can be used for both biological and chemical detection. Simultaneously, efforts are continuing in improving the performance of alternative cavities based on silicon, Si_xN_x, AlGaAs and polymers.[16, 36-39] Hence, over time, there will likely be many distinct device platforms on which ultra-high-Q biological and chemical sensors can be based.

ACKNOWLEDGEMENTS

The authors would like to thank Prof. Richard Flagan and Dr. Rajan Kulkarni, for numerous helpful discussions. A.M. Armani is supported by a Clare Boothe Luce Post-doctoral Fellowship. This work was supported by the DARPA Center for OptoFluidic Integration.

REFERENCES

[1] B. Alsina, T. Vu, and S. Cohen-Cory, "Visualizing synapse formation in arborizing optic axons in vivo: dynamics and modulation by BDNF," *Nature Neuroscience*, vol. 4, pp. 1093-1101, 2001.

[2] J. K. Jaiswal and S. M. Simon, "Imaging single events at the cell membrane," *Nature Chemical Biology*, vol. 3, pp. 92-98, 2007.

[3] S. Tavintharan, M. Sivakumar, S. C. Lim, and C. F. Sum, "Niacin affects cell adhesion molecules and plasminogen activator inhibitor-1 in HepG2 cells," *Clinica Chimica Acta*, vol. 376, pp. 41-44, 2007.

[4] E. G. Biondi, S. J. Reisinger, J. M. Skerker, M. Arif, B. S. Perchuk, K. R. Ryan, and M. T. Laub, "Regulation of the bacterial cell cycle by an integrated genetic circuit," *Nature*, vol. 444, pp. 899-904, 2006.

[5] A. M. Armani, R. P. Kulkarni, S. E. Fraser, R. C. Flagan, and K. J. Vahala, "Label-Free, Single-Molecule Detection with Optical Microcavities," *Science*, vol. 317, pp. 783 (2007). published online July 5, 2007 [DOI: 10.1126/science.1145002].

[6] R. W. Boyd and J. E. Heebner, "Sensitive disk resonator photonic biosensor," *Applied Optics*, vol. 40, pp. 5742-5747, 2001.

[7] A. Hoshino, K. Fujioka, N. Manabe, S. Yamaya, Y. Goto, M. Yasuhara, and K. Yamamoto, "Simultaneous multicolor detection system of the single-molecular microbial antigen with total internal reflection fluorescence microscopy," *Microbiology and Immunology*, vol. 49, pp. 461-470, 2005.

[8] R. A. Vijayendran and D. E. Leckband, "A quantitative assessment of heterogeneity for surface-immobilized proteins," *Analytical Chemistry*, vol. 73, pp. 471-480, 2001.

[9] C. Monat, P. Domachuk, B.J. Eggleton, "Integrated optofluidics: A new river of light," *Nature Photonics*, vol. 1, pp. 106-114, 2006.

[10] F. Vollmer, S. Arnold, D. Braun, I. Teraoka, and A. Libchaber, "Multiplexed DNA quantification by spectroscopic shift of two microsphere cavities," *Biophysical Journal*, vol. 85, pp. 1974-1979, 2003.

[11] J. Topolancik and F. Vollmer, "All-optical switching in the near infrared with bacteriorhodopsin-coated microcavities," *Applied Physics Letters*, vol. 89, pp. -, 2006.

[12] C. Y. Chao and L. J. Guo, "Biochemical sensors based on polymer microrings with sharp asymmetrical resonance," *Applied Physics Letters*, vol. 83, pp. 1527-1529, 2003.

[13] S. Y. Cho and N. M. Jokerst, "A polymer microdisk photonic sensor integrated onto silicon," *Ieee Photonics Technology Letters*, vol. 18, pp. 2096-2098, 2006.

[14] J. K. S. Poon, L. Zhu, G. A. DeRose, and A. Yariv, "Transmission and group delay of microring coupled-resonator optical waveguides," *Optics Letters*, vol. 31, pp. 456-458, 2006.

[15] A. Ksendzov and Y. Lin, "Integrated optics ring-resonator sensors for protein detection," *Optics Letters*, vol. 30, pp. 3344-3346, 2005.

[16] A. M. Armani, A. Srinivasan, K. J. Vahala, "Soft Lithographic Fabrication of High Q Polymer Microcavity Arrays," *Nano Letters*, vol. 7, 2007.

[17] J. Yang and L. J. Guo, "Optical sensors based on active microcavities," *Ieee Journal of Selected Topics in Quantum Electronics*, vol. 12, pp. 143-147, 2006.

[18] S. Blair and Y. Chen, "Resonant-enhanced evanescent-wave fluorescence biosensing with cylindrical optical cavities," *Applied Optics*, vol. 40, pp. 570-582, 2001.

[19] M. Steiner, F. Schleifenbaum, C. Stupperich, A. V. Failla, A. Hartschuh, and A. J. Meixner, "A new microcavity design for single molecule detection," *Journal of Luminescence*, vol. 119, pp. 167-172, 2006.

[20] S. Arnold, M. Khoshsima, I. Teraoka, S. Holler, and F. Vollmer, "Shift of whispering-gallery modes in microspheres by protein adsorption," *Optics Letters*, vol. 28, pp. 272-274, 2003.

[21] M. L. Gorodetsky, A. A. Savchenkov, and V. S. Ilchenko, "Ultimate Q of optical microsphere resonators," *Optics Letters*, vol. 21, pp. 453-455, 1996.

[22] D. W. Vernooy, V. S. Ilchenko, H. Mabuchi, E. W. Streed, and H. J. Kimble, "High-Q measurements of fused-silica microspheres in the near infrared," *Optics Letters*, vol. 23, pp. 247-249, 1998.
[23] H. Rokhsari, S. M. Spillane, and K. J. Vahala, "Loss characterization in microcavities using the thermal bistability effect," *Applied Physics Letters*, vol. 85, pp. 3029-3031, 2004.
[24] Y. Z. Yang, P. Li, S. H. Dai, D. C. Wu, R. X. Li, J. H. Yang, and H. B. Xiao, "The measurement and analysis of visible-absorption spectrum and fluorescence spectrum of lycopene," *Spectroscopy and Spectral Analysis*, vol. 25, pp. 1830-1833, 2005.
[25] P. Heimala, P. Katila, J. Aarnio, and A. Heinamaki, "Thermally tunable integrated optical ring resonator with poly-Si thermistor," *Journal of Lightwave Technology*, vol. 14, pp. 2260-2267, 1996.
[26] D. Armani, B. Min, A. Martin, and K. J. Vahala, "Electrical thermo-optic tuning of ultrahigh-Q microtoroid resonators," *Applied Physics Letters*, vol. 85, pp. 5439-5441, 2004.
[27] D. K. Armani, T. J. Kippenberg, S. M. Spillane, and K. J. Vahala, "Ultra-high-Q toroid microcavity on a chip," *Nature*, vol. 421, pp. 925-928, 2003.
[28] A. M. Armani, D. K. Armani, B. Min, K. J. Vahala, and S. M. Spillane, "Ultra-high-Q microcavity operation in H_2O and D_2O," *Applied Physics Letters*, vol. 87, pp. 151118, 2005.
[29] A. L. Martin, D. K. Armani, L. Yang, and K. J. Vahala, "Replica-molded high-Q polymer microresonators," *Optics Letters*, vol. 29, pp. 533-535, 2004.
[30] S. M. Spillane, T. J. Kippenberg, O. J. Painter, and K. J. Vahala, "Ideality in a fiber-taper-coupled microresonator system for application to cavity quantum electrodynamics," *Physical Review Letters*, vol. 91, pp. -, 2003.
[31] M. Cai, O. Painter, and K. J. Vahala, "Observation of critical coupling in a fiber taper to a silica-microsphere whispering-gallery mode system," *Physical Review Letters*, vol. 85, pp. 74-77, 2000.
[32] L. A. Klumb, V. Chu, and P. S. Stayton, "Energetic roles of hydrogen bonds at the ureido oxygen binding pocket in the streptavidin-biotin complex," *Biochemistry*, vol. 37, pp. 7657-7663, 1998.
[33] B. Mazur, A. Mertas, D. Sonta-Jakimczyk, T. Szczepanski, and A. Janik-Moszant, "Concentration of IL-2, IL-6, IL-8, IL-10 and TNF-alpha in children with acute lymphoblastic leukemia after cessation of chemotherapy," *Hematological Oncology*, vol. 22, pp. 27-34, 2004.
[34] G. Subramania, S. Y. Lin, J. R. Wendt, and J. M. Rivera, "Tuning the microcavity resonant wavelength in a two-dimensional photonic crystal by modifying the cavity geometry," *Applied Physics Letters*, vol. 83, pp. 4491-4493, 2003.
[35] S. G. Kim, C. W. Wong, and Y. B. Jeon, "Strain-tuning of optical devices with nanometer resolution," *Cirp Annals-Manufacturing Technology*, vol. 52, pp. 431-434, 2003.
[36] M. Borselli, T. J. Johnson, and O. Painter, "Beyond the Rayleigh scattering limit in high-Q silicon microdisks: theory and experiment," *Optics Express*, vol. 13, pp. 1515-1530, 2005.
[37] P. E. Barclay, K. Srinivasan, O. Painter, B. Lev, and H. Mabuchi, "Integration of fiber-coupled high-Q SiNx microdisks with atom chips," *Applied Physics Letters*, vol. 89, pp. -, 2006.
[38] K. Srinivasan, M. Borselli, and O. Painter, "Cavity Q, mode volume, and lasing threshold in small diameter AlGaAs microdisks with embedded quantum dots," *Optics Express*, vol. 14, pp. 1094-1105, 2006.
[39] C. P. Michael, K. Srinivasan, T. J. Johnson, O. Painter, K. H. Lee, K. Hennessy, H. Kim, and E. Hu, "Wavelength- and material-dependent absorption in GaAs and AlGaAs microcavities," *Applied Physics Letters*, vol. 90, pp. -, 2007.